Proc. Natl. Acad. Sci. USA
Vol. 87, pp. 5084–5088, July 1990
Physiology

Real-time imaging of calcium influx in mammalian cerebellar Purkinje cells *in vitro*

(calcium spike/Fura-2/dendritic spike/plateau potential/glutamate response)

MUTSUYUKI SUGIMORI AND RODOLFO R. LLINÁS

Department of Physiology and Biophysics, New York University Medical Center, 550 First Avenue, New York, NY 10016

Contributed by Rodolfo R. Llinás, April 18, 1990

ABSTRACT **Real-time visualization of intracellular calcium concentration ($[Ca^{2+}]_i$) changes in mammalian Purkinje cells *in vitro*, utilizing the dye Fura-2, indicates that calcium action potentials are generated in the dendritic tree and follow a particular activation sequence. During spontaneous oscillations or after direct current injection, dendritic spikes are initiated as slow and graded plateau potentials at the level of the tertiary or spiny branchlets of the dendrite. As the plateau potentials become sufficiently high to reach the firing threshold for full dendritic spike generation, calcium entry is observed at the more proximal branches of the dendritic tree. These action potentials are then conducted orthodromically toward the soma and may invade other branches in the arbor antidromically. Simultaneous recording of the intracellular electrical activity and the Fura-2 fluorescent signal indicates that the intracellular calcium transients are accompanied by a very rapid increase in intracellular calcium concentration. This increase in $[Ca^{2+}]_i$ exhibits an almost equally fast return to baseline after the termination of the action potential, indicating the presence of very efficient calcium sequestering and extruding mechanisms in the dendrites. Iontophoretic application of glutamate at the dendritic level provided a further demonstration of the spatial separation of plateau potentials from dendritic spikes and gives further insights into the details of dendritic integration in this neuron.**

The presence of voltage-dependent calcium conductances capable of generating dendritic spikes in cerebellar Purkinje cells has been postulated on electrophysiological grounds in avian (1), mammalian (2, 3), and reptilian (4) species. However, a direct demonstration of the localization and time course of the intracellular calcium concentration ($[Ca^{2+}]_i$) transients underlying these spikes has not been obtained with sufficient spatial resolution to determine the exact distribution of calcium influx over the soma–dendritic membrane. Indeed, while the existence of dendritic calcium conductances proposed on electrophysiological grounds has been confirmed by using the fluorescence dye Arsenazo II (5), the methodology used has some significant limitations. Measurements were obtained by using a 12 × 12 matrix photodiode with an excellent time response; however, the precise spatial localization of the calcium entry into the dendritic tree could not be accurately resolved because of the small number of photodiodes. Recently, using Fura-2 (6), a more precise image of the calcium transients in Purkinje cells was achieved (7, 8). However, in this case the time resolution was 250 msec per image, which falls short of the temporal resolution required for a detailed description of the steps in the generation of dendritic calcium spikes.

Here we report results obtained with an imaging system capable of measuring the reduction of Fura-2 fluorescence during calcium entry with a spatial resolution of 512 × 483 pixels at a rate of 200 or 400 frames per sec. At this speed, a dendritic calcium spike, which lasts 10–20 msec, can be captured in four to eight frames and the spatial and temporal distribution of the calcium transient can be followed accurately.

MATERIALS AND METHODS

The experiments were performed in cerebellar slices from adult guinea pigs. The tissue preparation and intracellular recording techniques are the same as those used in previous experiments from our laboratory (2). After somatic penetration of the Purkinje cell, Fura-2 [10 mM solution of the pentapotassium salt (Molecular Probes)] was iontophoretically injected for 15–30 min with a −0.5-nA constant current (Instrument IR-283, NeuroData, New York). After loading with Fura-2, the impaled neuron demonstrated a powerful fluorescent signal with 380-nm excitation (Fig. 1*B*).

High-Speed Imaging of Fura-2 Signal. To reduce the phototoxicity and dye bleaching to a minimum the tissue was illuminated at low power and the fluorescent image was electronically intensified (VIM camera, Hamamatsu Photonics, Hamamatsu, Japan) and stored by using a high-speed video system (HSV-400, nac Inc., Tokyo) (Fig. 1*A*). The electrical activity recorded from the Purkinje cell soma was recorded simultaneously with the image by using a "wave inserter" (nac Inc. V-907-W). Because of the high speed with which the recordings were obtained, the absolute calcium concentrations could not be calculated by the 340/380-nm fluorescence ratio method (6, 9). Rather, the images of $[Ca^{2+}]_i$ were obtained with excitation at 380 nm by subtracting the image during activity from the image stored prior to activation (10). Because the ratio method was not used, the values for $[Ca^{2+}]_i$ are qualitative. This on-line subtraction was implemented via a Hamamatsu color video signal processor (model C1966) through the NTSC video signal output of the HSV-400 (Fig. 1*A*) allowing 60 levels of gray to be resolved (Fig. 1 *B* and *C*). Thus, with a better color processor more color levels may be resolved than are shown in Figs. 2–4. Images could be played back in slow motion such that frames taken at 200 or 400 per sec were viewed at 30 per sec.

RESULTS

Imaging of Calcium Spikes. Purkinje cell action potentials obtained from adult guinea pig cerebellum were recorded after depolarization of the neurons with transmembrane current pulses, during spontaneous oscillations, or after iontophoretic application of glutamic acid at dendritic level.

The instrumentation required to visualize Fura-2-injected Purkinje cells with light excitation at 380 nM is illustrated in Fig. 2*A*. Fig. 2*B* represents the image obtained after on-line

The publication costs of this article were defrayed in part by page charge payment. This article must therefore be hereby marked "*advertisement*" in accordance with 18 U.S.C. §1734 solely to indicate this fact.

Abbreviation: $[Ca^{2+}]_i$, intracellular calcium concentration.

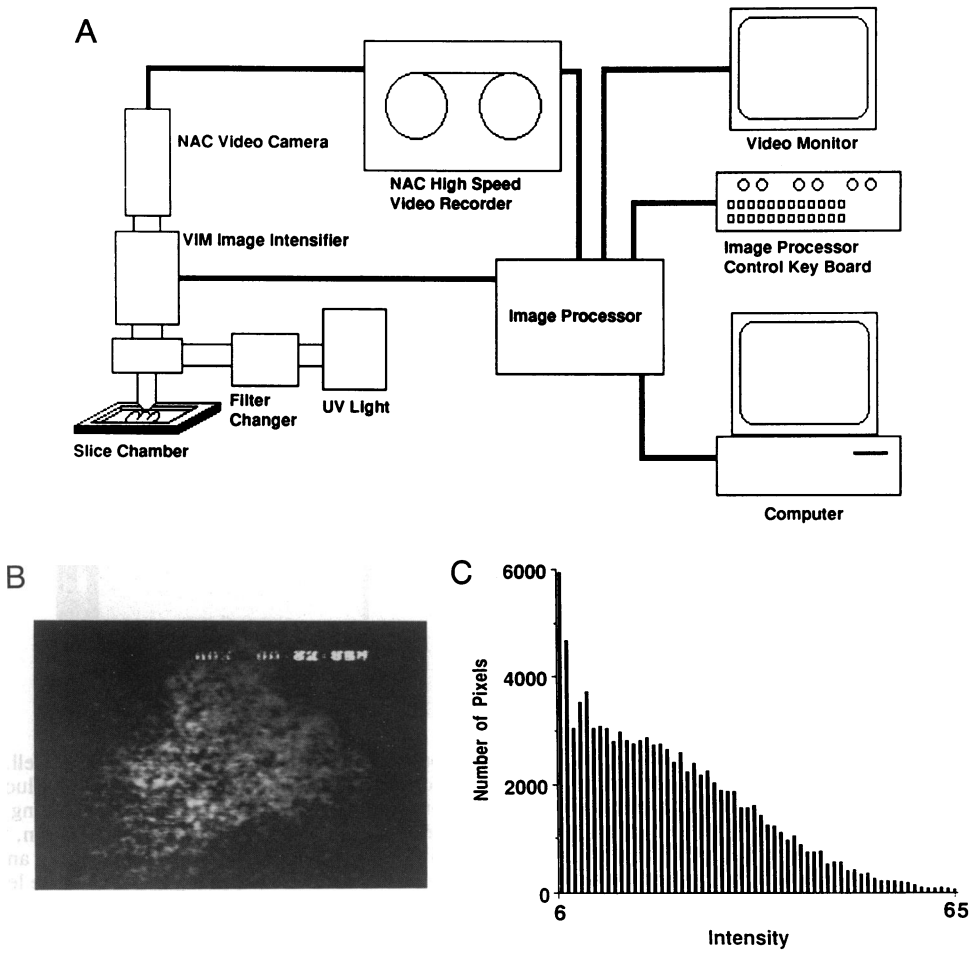

FIG. 1. Fura-2 imaging technique. (*A*) Imaging system (from left to right): recording chamber with UV epi-illumination microscope and filter carrier system to activate and visualize the dye in the injected Purkinje cell. Fluorescence is intensified by the VIM (maximum gain, 1×10^6; phosphor decay time constant, 200 μsec). The image is recorded by a nac high-speed video camera (with Plumbicon tubes), which feeds the nac high-speed videotape recorder (capable of storing 200 or 400 frames per sec). The frames are subtracted in real time by an image processor, which gives an image of the difference between the resting and reduced fluorescence due to increased $[Ca^{2+}]_i$. The image processor can address the video monitor and graphic analysis computer. (*B*) A 512 × 483 pixel display of a fine-grain black and white subtracted image showing $[Ca^{2+}]_i$ in a Purkinje cell dendrite (same cell as in Fig. 2). (*C*) A gray level intensity histogram of the image in *B* showing a resolution of ≈60 gray levels. Abscissa, intensity level in arbitrary units from a range of 0 to 255 (8 bits).

subtraction of the fluorescence of the injected Purkinje cell from the averaged (n = 16 frames) background fluorescence (obtained during an electrically silent period just prior to activation). Entry of calcium during the plateau potential that preceded dendritic calcium spike activation (3) was most prominent in the periphery of the dendritic tree (Fig. 2*C*), while increased $[Ca^{2+}]_i$ was not seen in the main dendrites until the initial peak of a calcium spike (Fig. 2*D*). Subsequent action potentials occurred in different branches of the Purkinje cell (Fig. 2 *E–G*). The image in Fig. 2*H* was taken at a time of intermediate activity between dendritic spikes. In Fig. 2*I*, dendritic spiking abruptly ceased and $[Ca^{2+}]_i$ returned to control levels. Note that the increase in calcium concentration occurred initially at the fine dendritic branches and that during repetitive activity some dendritic branches showed larger signals than others. This is to be expected given the noncontinuous nature of dendritic spike conduction, as demonstrated in reptilian (11) and mammalian (3) Purkinje cells.

Direct Correlation of Calcium Spikes and Fura-2 Images. Simultaneous recording of the fluorescent signal and somatic electrical responses during direct stimulation of the neuron is illustrated in Fig. 3. The intracellular recordings (left) are displayed vertically from the top to the bottom on the video monitor (Fig. 3 *A–C*). Thus, the uppermost point in the vertical scan (arrowheads in *A–C*) corresponds to the time at which the image displayed on the video monitor was recorded.

The distribution of $[Ca^{2+}]_i$ in a dendrite immediately before calcium spike generation (during the plateau potential) demonstrates a low level of fluorescence (Fig. 3*A*). In the next frame, recorded 5 msec later, the action potential had reached its peak and was in its falling phase (Fig. 3*B*). Note the increase in the Fura-2 signal spread over most of the dendritic tree to include the main dendritic branches. The third frame (Fig. 3*C*), taken 5 msec later, shows the fluorescence at the end of the action potential. At that time, the Fura-2 signal was sharply reduced. A clear picture of the difference between the fluorescence signal immediately before (Fig. 3*D*) and at the initial portion of the falling phase of the calcium spike (Fig. 3*E*) was obtained by image averaging. Thus, rather than showing a single spike event at these different time points as shown in Fig. 3 *A–C*, the images shown in Fig. 3 *D* and *E* are averages of 12 frames taken 5 msec before and at the initiation of the falling phase of the spike, respectively. The moment during the action potential at which each of the 12 images was taken is also shown [Fig. 3 *D* and *E* (*Insets*)]. The spikes in Fig. 3*D* were selected such that an image frame was recorded 5 msec before their peak. Each image that contributed to the average in Fig. 3*E* was

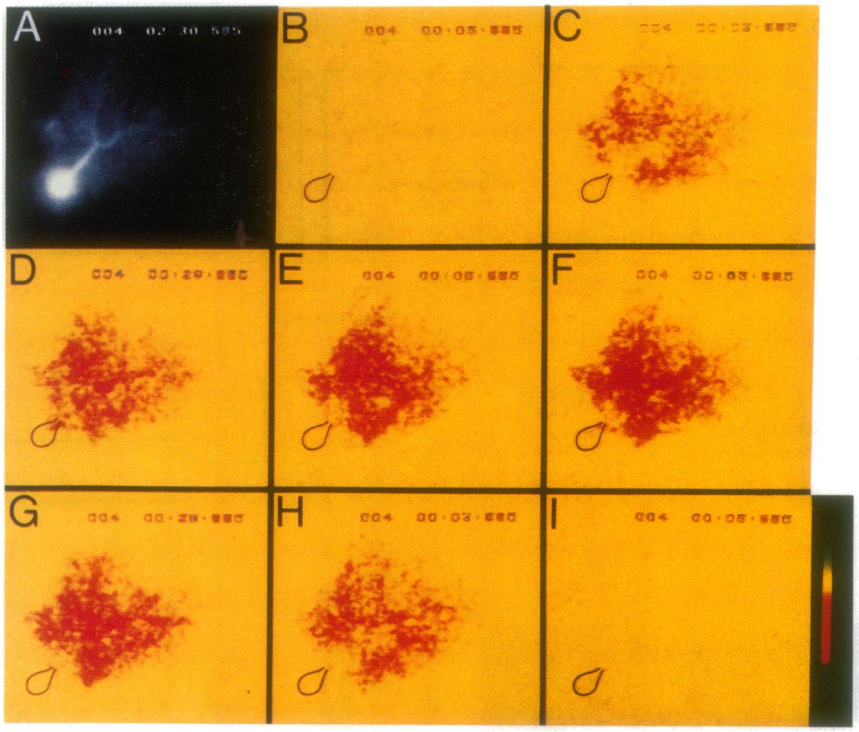

FIG. 2. Illustration of different levels and locations of $[Ca^{2+}]_i$ during spontaneous dendritic spiking in a Purkinje cell. In this as well as in Figs. 3 and 4, the body of the Purkinje cell has been drawn to mark its location with respect to the Fura-2 signal. (*A*) Fluorescent image of the neuron after removing the intracellular electrode. (*B*) Subtraction of background fluorescence from continuous recording showing no increase in $[Ca^{2+}]_i$ at the resting potential. (*C*) $[Ca^{2+}]_i$ at the beginning of the burst prior to dendritic action potential generation, the so-called plateau potential. (*D–H*) Fluctuations of fluorescence in the dendritic tree during activity. (*E–G*) Full dendritic spikes occurred and were accompanied by increased $[Ca^{2+}]_i$ in the main dendrites. (*H*) Intermediate time between spikes. (*I*) Return of $[Ca^{2+}]_i$ to the baseline level after termination of dendritic spike burst. The color bars in this figure and in Fig. 3 (*A–C*) indicate a reduction of fluorescence (increased $[Ca^{2+}]_i$) from yellow to red and in Fig. 4 increases in $[Ca^{2+}]_i$ are indicated from red to green.

taken at the onset of the falling phase of the action potential (see *Inset*). Note that the difference in the Fura-2 signal at these two instants corroborates the difference shown in Fig. 3 *A* and *B*. Fig. 3*F* shows the Purkinje cell (and the recording electrode) during a period of inactivity (the vertical line to the left indicates the resting membrane potential).

Dendritic Glutamate Iontophoresis. The distribution of $[Ca^{2+}]_i$ after iontophoretic application of glutamate to the

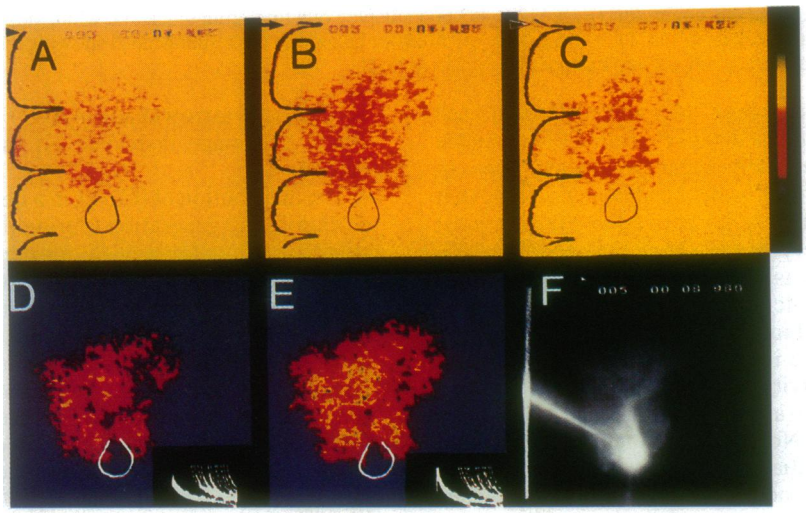

FIG. 3. Simultaneous recordings of the fluorescent signal and the electrical responses recorded at the somatic level. (*A–C*) Three successive frames taken at 5-msec intervals from the beginning of the plateau phase to the return to the resting membrane potential after a dendritic spike. (*A*) Distribution of $[Ca^{2+}]_i$ in a dendrite immediately prior to the dendritic calcium spike (plateau potential). Time zero for every frame corresponds to the beginning (arrow) of the vertical voltage trace shown to the left of each frame. (The action potential moves downward with time.) (*B*) Change of the Fura-2 signal immediately after the peak of the calcium spike. (*C*) $[Ca^{2+}]_i$ changes 5 msec after the action potential peak. (*D* and *E*) The difference in the Fura-2 signal was determined by averaging 12 images, which were acquired at the same point in time during successive dendritic spikes as the images in *A–C*. (*D*) Plateau potential 5 msec before the peak of the calcium spike. (*E*) $[Ca^{2+}]_i$ distribution 5 msec later immediately after the peak of the action potential. Note that the averages corroborate the results obtained from the signal traces. (*F*) Photograph of the dye-injected Purkinje cell shown in *A–E* demonstrating the fluorescent images of the intrasomatic electrode (subtracted out in *A–E*) and the resting membrane potential level (vertical line on the left). Calibration (in Fig. 4*C*) was 30 mV, 5 msec.

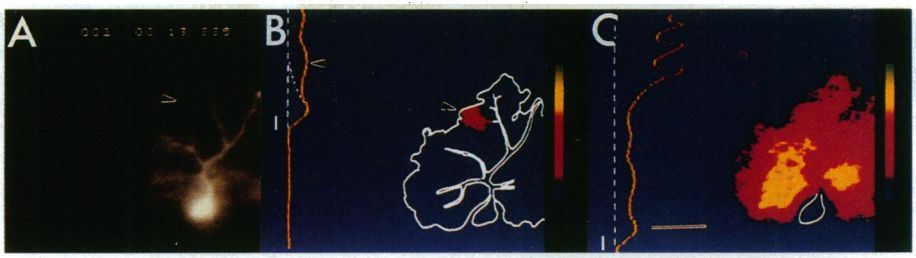

FIG. 4. Distribution of $[Ca^{2+}]_i$ after iontophoretic application of glutamate to the dendrite of a Purkinje cell following Fura-2 loading. (*A*) The fluorescent cell (arrowhead marks the position of the iontophoretic electrode). (*B*) Iontophoresis producing a plateau potential (left-pointing arrow) after the initial ligand-dependent depolarization. (The dendritic tree was drawn in white to mark its location with respect to the Fura-2 signal.) During the plateau potential, a distinct increase of $[Ca^{2+}]_i$ was observed at the dendritic branchlet level (right-pointing arrow). Increased $[Ca^{2+}]_i$ was not observed in the absence of a plateau potential. (*C*) The plateau potential was followed by full dendritic spiking. Note that the $[Ca^{2+}]_i$ increase, although widespread, was highest in the three lower main dendrites. Calibration was 30 mV, 5 msec.

Purkinje cell dendrites is shown in Fig. 4. Fig. 4*A* (arrowhead) marks the position of the iontophoretic electrode with respect to the Fura-2 loaded cell. As shown in Fig. 4*B*, iontophoresis of glutamate elicited a plateau potential (left-pointing arrow) during which distinct calcium entry was observed at the level of the dendritic branchlets (right-pointing arrow). In cases in which the ligand-dependent depolarization did not generate a plateau potential (waveform indicated by the dots in Fig. 4*B*), no calcium entry was observed. When the plateau potential elicited full dendritic spiking (Fig. 4*C*), widespread calcium entry was particularly prominent in the main dendrites (yellow and green).

These results indicate that glutamate iontophoresis activates the spiny branchlets, which generate maximal amplitude responses via the opening of voltage-dependent calcium channels in these fine processes. It is these responses that are seen at the somatic level as plateau potentials. When a sufficient number of branchlets are depolarized to bring the plateau potential to the threshold for spike initiation, the secondary dendritic branches generate full spikes. These spikes propagate orthodromically toward the soma and antidromically into other distal dendritic branchlets, producing an image such as that shown in Fig. 4*C*.

DISCUSSION

These data illustrate the time course of intracellular free calcium transients during activity in a mammalian neuron in real time. Given the speed with which the Fura-2 signal occurs after an action potential, the most parsimonious explanation for these images is that they correspond to the site of calcium influx—i.e., to the plasmalemmal localization of voltage-dependent calcium channels. From this point of view, the present study corroborates previous physiological and imaging studies that indicate that calcium conductances are localized in the Purkinje cell dendrites (1–5, 7, 8).

Perhaps our most surprising finding was the speed with which the $[Ca^{2+}]_i$ increased and then returned to baseline levels in the dendritic tree. Indeed, our results indicate a period as short as 10 msec for the return phase, suggesting that the cytosol of the thinner dendritic branches is capable of controlling calcium concentration increases in an extraordinarily short time. The second finding, which had not been previously observed in fluorescent dye imaging, was the tendency of Purkinje cells to generate all-or-none spikes in each of the main branches of the dendritic tree independently. Thus, in the three examples shown here and in the 11 other cells recorded, action potentials could fire in each of the dendritic branches separately. On occasion, as the cell became more depolarized the whole dendritic tree fired in a close to synchronous manner.

Under these experimental conditions, all cells studied demonstrated clear calcium concentration changes only in the dendritic tree, very much in keeping with the electrophysiological findings indicating that in the adult Purkinje cells somatic calcium entry is minimal (2, 8, 12). This point is critical, since several studies have indicated that calcium may enter the soma of Purkinje cells after cell dissociation or in culture (9, 13). This is in keeping with results previously described (14) on the generation of calcium action potentials during development. Thus, in a 4-day-old Purkinje cell, which has immature, short dendrites, powerful calcium spikes have been recorded at the somatic level (14). However, such events have not been seen in slices of mature Purkinje cells. This suggests that during maturation or after the lesion of a major dendritic branch, somatic calcium conductances may be observed since growth cones exhibit voltage-dependent calcium conductances and even full calcium-dependent action potentials (15, 16).

The dendritic localization of voltage-dependent calcium channels, especially in the tertiary and spiny branchlets, may be related to the particular distribution and synaptic organization of the two types of Purkinje cell afferents. The parallel fibers represent the majority of the synaptic input to the Purkinje cell with as many as 2×10^5 junctions. They terminate on the spine heads of the spiny branchlets of the distalmost portion of the dendritic tree, and so, to play a significant role in cell excitability, dendritic electroresponsiveness may serve to enhance such synaptic potentials. This can be implemented by the calcium channels in the spiny branchlets, which could give rise to plateau potentials without compromising the integrative ability of the Purkinje cell. By contrast, the climbing fiber input, which generates a clear calcium spike burst (2, 3), does so by activating directly the main portion of the dendritic tree, where such spikes are generated.

This investigation was supported by Grant NS13742 from the National Institute of Neurological Disorders and Stroke.

1. Llinás, R. & Hess, R. (1976) *Proc. Natl. Acad. Sci. USA* **73,** 2520–2523.
2. Llinás, R. & Sugimori, M. (1980) *J. Physiol. (London)* **305,** 171–195.
3. Llinás, R. & Sugimori, M. (1980) *J. Physiol. (London)* **305,** 197–213.
4. Hounsgaard, J. & Midtgaard, J. (1988) *J. Physiol. (London)* **402,** 731–749.
5. Ross, W. N. & Werman, R. (1987) *J. Physiol. (London)* **389,** 319–336.
6. Tsien, R. Y. & Poeni, M. (1986) *Trends Biochem. Sci.* **11,** 450–455.
7. Tank, D. W., Sugimori, M., Connor, J. A. & Llinás, R. (1988) *Science* **242,** 773–777.
8. Hockberg, P. E., Tseng, H. Y. & Connor, J. A. (1989) *J. Neurosci.* **9,** 2272–2284.
9. Connor, J. A. & Tseng, H. Y. (1988) *Brain Res. Bull.* **21,** 353–361.

10. Sugimori, M. & Llinás, R. (1989) *Soc. Neurosci. Abstr.* **15,** 179.
11. Llinás, R. & Nicholson, C. (1971) *J. Neurophysiol.* **34,** 532–551.
12. Sugimori, M. & Llinás, R. (1984) *Soc. Neurosci. Abstr.* **10,** 659.
13. Gruol, D. L. & Franklin, C. L. (1987) *J. Neurosci.* **7,** 1271–1293.
14. Llinás, R. & Sugimori, M. (1979) *Prog. Brain Res.* **51,** 323–334.
15. Macvicar, B. A. & Llinás, R. R. (1985) *J. Neurosci. Res.* **13,** 323–336.
16. Connor, J. A., Kater, S. B., Cohen, C. & Fink, L. (1990) *Cell Calcium* **11,** 233–239.